

# Hypoiodous Acid as Guest Molecule in Protonated Water Clusters: A Combined FT-ICR/DFT Study of $I(H_2O)_n^+$

Uwe Achatz, Brigitte S. Fox, Martin K. Beyer, and Vladimir E. Bondybey\*

Contribution from the Institut für Physikalische und Theoretische Chemie, Technische Universität München, Lichtenbergstrasse 4, 85747 Garching, Germany

Received February 12, 2001

**Abstract:** Cationic water clusters containing iodine, of the composition  $I(H_2O)_n^+$ ,  $n = 0-25$ , are generated in a laser vaporization source and investigated by FT-ICR mass spectrometry. An investigation of blackbody radiation-induced fragmentation of size-selected clusters  $I(H_2O)_n^+$ ,  $n = 3-15$ , under collision-free conditions revealed an overall linear increase of the unimolecular rate constant with cluster size, similar to what has been observed previously for other hydrated ions. Above a certain critical size,  $I(H_2O)_n^+$ ,  $n \geq 13$ , reacts with HCl by formation of the interhalide ICl and a protonated water cluster, which is the reverse of a known solution-phase reaction. Accompanying density functional calculations illustrate the conceptual differences between cationic and anionic iodine–water clusters  $I(H_2O)_n^\pm$ . While  $I^-(H_2O)_n$  is genuinely a hydrated iodide ion, the cationic closed-shell species  $I(H_2O)_n^+$  may be best viewed as a protonated water cluster, in which one water molecule is replaced by hypoiodous acid. In the strongly acidic environment, HOI is protonated because of its high proton affinity. However, similar to the well-known  $H_3O^+/H_5O_2^+$  controversy in protonated water clusters, a smooth transition between  $H_2IO^+$  and  $H_4IO_2^+$  as core ions is observed for different cluster sizes.

## 1. Introduction

Chlorides are the most abundant anions in seawater; other halides also occur in appreciable concentrations. Aerosols originating from seawater are also believed to be one of the major sources of halogens in the atmosphere. Ionic water clusters containing halogens are suitable, simplified model systems for aerosol studies, and it is therefore not surprising that they have been extensively investigated both experimentally<sup>1–8</sup> and theoretically.<sup>9–14</sup>

For small systems such as  $X^-(H_2O)$  ( $X = F, Cl, Br, I$ ), spectroscopic data exist. Vibrational predissociation spectroscopy studies by Bailey et al.<sup>15</sup> and Okumura and co-workers<sup>16</sup>

suggested that the water molecule in  $I^-(H_2O)$  forms a single hydrogen bond to the iodide anion. For larger solvated systems, the situation is not so clear. The questions of whether the halide is inside the clusters or on their surface, and how many water molecules are necessary for its complete solvation, are among the hotly discussed topics in halogen hydration. Most of the published studies deal with anionic halide–water species.

Using the FT-ICR technique with an efficient external source, one can study solution chemistry in finite clusters and gain a microscopic, molecular-scale understanding. An interesting and useful common property of all hydrated clusters is that even in the collision-free environment of the FT-ICR instrument, they gradually fragment due to absorption of the blackbody infrared radiation from the room-temperature apparatus walls.<sup>17–23</sup> One finds that for most such hydrated systems, for instance  $Al^+(H_2O)_n$ ,  $Mg^+(H_2O)_n$ , or  $Ag^+(H_2O)_n$  with metal core ions, the fragmentation rates are roughly proportional to the number of ligands and, consequently, the number of infrared absorbers.<sup>21–23</sup>

We have recently examined fragmentation of the  $I^-(H_2O)_n$  anions and their reactions with HCl using Fourier transform ion cyclotron resonance mass spectrometry (FT-ICR).<sup>1</sup> While it is not to be expected that hydrated iodine cations, with  $I^+$  in its triplet ground state, would be of great chemical relevance,

\* To whom correspondence should be addressed. Tel.: ++49-89-289-13420. Fax: ++49-89-289-13416. E-mail: bondybey@ch.tum.de.

(1) Achatz, U.; Joos, S.; Berg, C.; Beyer, M.; Niedner-Schatteburg, G.; Bondybey, V. E. *Chem. Phys. Lett.* **1998**, *291*, 459.

(2) Arshadi, M.; Yamdagni, R.; Kebarle, P. *J. Phys. Chem.* **1970**, *74*, 1475.

(3) Hiraoka, K.; Misuze, S.; Yamabe, S. *J. Phys. Chem.* **1988**, *92*, 3943.

(4) Zook, G. R.; Grimsrud, E. P. *Int. J. Mass Spectrom. Ion Processes* **1991**, *107*, 293.

(5) Schindler, T.; Berg, C.; Niedner-Schatteburg, G.; Bondybey, V. E. *Chem. Phys. Lett.* **1994**, *229*, 57.

(6) Beyer, M.; Berg, C.; Goerlitzer, H. W.; Schindler, T.; Achatz, U.; Albert, G.; Niedner-Schatteburg, G.; Bondybey, V. E. *J. Am. Chem. Soc.* **1996**, *118*, 7386.

(7) Achatz, U.; Joos, S.; Berg, C.; Schindler, T.; Beyer, M.; Albert, G.; Niedner-Schatteburg, G.; Bondybey, V. E. *J. Am. Chem. Soc.* **1998**, *120*, 1876.

(8) Fox, B. S.; Beyer, M.; Achatz, U.; Joos, S.; Niedner-Schatteburg, G.; Bondybey, V. E. *J. Phys. Chem. A* **2000**, *104*, 1147.

(9) Lybrand, T. P.; Kollman, P. A. *J. Chem. Phys.* **1985**, *83*, 2923.

(10) Sung, S.-S.; Jordan, P. C. *J. Chem. Phys.* **1986**, *85*, 4045.

(11) Lin, S.; Jordan, P. C. *J. Chem. Phys.* **1988**, *89*, 7492.

(12) Dang, L. X.; Garret, B. C. *J. Chem. Phys.* **1993**, *99*, 2972.

(13) Gai, H.; Schenter, G. K.; Dang, L. X.; Garret, B. C. *J. Chem. Phys.* **1996**, *105*, 8835.

(14) Xantheas, S. S. *J. Phys. Chem.* **1996**, *100*, 9703.

(15) Bailey, C. G.; Kim, J.; Dessent, C. E. H.; Johnson, M. A. *Chem. Phys. Lett.* **1997**, *269*, 122.

(16) Johnson, M. S.; Kuwata, K. T.; Wong, C.-K.; Okumura, M. *Chem. Phys. Lett.* **1996**, *260*, 551.

(17) Thoelmann, D.; Tonner, D. S.; McMahon, T. B. *J. Phys. Chem.* **1994**, *98*, 2002.

(18) Dunbar, R. C. *J. Phys. Chem.* **1994**, *98*, 8705.

(19) Sena, M.; Riveros, J. M. *Rapid Commun. Mass Spectrom.* **1994**, *8*, 1031.

(20) Schnier, P. D.; Price, W. D.; Jockusch, R. A.; Williams, E. R. *J. Am. Chem. Soc.* **1996**, *118*, 7178.

(21) Schindler, T.; Berg, C.; Niedner-Schatteburg, G.; Bondybey, V. E. *Chem. Phys. Lett.* **1996**, *250*, 301.

(22) Beyer, M.; Achatz, U.; Berg, C.; Joos, S.; Niedner-Schatteburg, G.; Bondybey, V. E. *J. Phys. Chem. A* **1999**, *103*, 671.

(23) Fox, B. S.; Beyer, M. K.; Bondybey, V. E., *J. Chem. Phys. A*, in press.

it is still an intriguing question whether a cluster of the composition  $I(H_2O)_n^+$  would exist and how it would behave. If the clusters had a singlet ground state, one could also formulate them as  $H^+(H_2O)_{n-1}(HOI)$ , that is, as a protonated water cluster in which one water molecule is replaced by hypoiodous acid. Cationic iodine containing water clusters therefore could be a promising candidate for studying the chemistry of hypoiodous acid in a strongly acidic environment.

Starting with the computational work by Glukhovtsev et al.<sup>24</sup> on their acidities and proton affinities, hypohalous acids have attracted growing attention in the physical chemistry community.<sup>25–29</sup> Given the relevance of hypohalous acids for atmospheric chemistry,<sup>24</sup> we considered it worthwhile to examine the properties of potentially HOX-containing clusters in our FT-ICR mass spectrometer. This paper reports our experimental and computational results with  $I(H_2O)_n^+$  clusters.

## 2. Experimental and Computational Details

The experiments were performed on a modified FT-ICR mass spectrometer, Spectrospin CMS47X,<sup>30</sup> equipped with an external molecular ion beam source, a 4.7-T superconducting magnet, and a 60- × 60-mm cylindrical “infinity” cell.<sup>31</sup>  $I(H_2O)_n^+$  clusters were produced in a disk-type laser vaporization source.<sup>32,33</sup> Compressed sodium iodide (Merck, 99.5%+) was vaporized with the focused 532-nm radiation of a Nd:YAG laser Continuum Surelight II operating at 10 Hz, with typically 10 mJ pulse energy in 5-ns pulses producing the initial plasma. The laser vaporization was synchronized with pulses of helium carrier gas seeded with water vapor, which were supplied by a home-built piezoelectric valve with 50 μs opening time. Typical pressures of water and helium are 35 mbar and 10 bar, respectively. The salt plasma entrained in the helium–water pulse was subsequently cooled by flowing through a confining channel and by subsequent supersonic expansion into high vacuum, resulting in cluster formation. The cluster ions were transferred into the high-field region of the superconducting magnet by a system of electrostatic lenses and stored inside the ICR cell. To improve the cluster ion signals, up to 20 injection cycles were accumulated at the 10 Hz repetition rate of the Nd:YAG laser, prior to the reaction delay and detection.

Cluster fragmentation was studied at a pressure of about  $4 \times 10^{-10}$  mbar, which corresponds to about one collision with the residual gas on the order of 100 s. Under these conditions, the clusters gradually fragment due to absorption of the blackbody infrared radiation from the ambient-temperature apparatus walls. The temperature of the vacuum tube enclosing the ICR cell was kept at a nearly constant value of  $T = 291 \pm 5$  K with the help of water flowing through the cooling jacket. Fragmentation rate constants were determined by fitting the observed decay of the signal of the size selected ion as a function of reaction time to the first-order reaction kinetics. To investigate reactions of the clusters with hydrogen chloride, the reactant HCl gas (Aldrich, 99%+) was used without further purification and introduced into the ultrahigh-vacuum region via a needle valve, maintaining a constant pressure of about  $1.0 \times 10^{-8}$  mbar.

All calculations were carried out on either an SGI Power Challenge or a DEC Alpha Station 500 using the three-parameter hybrid Hartree–

Fock/density functional (B3LYP) method described by Becke<sup>34,35</sup> as implemented in the Gaussian94<sup>36</sup> program package. For oxygen and hydrogen, the 6-311++G(3d,3pd) basis set, treating explicitly all electrons with two diffuse and three polarization functions, was employed. For iodine, the quasi-relativistic effective core potential basis set of the Stuttgart/Dresden group<sup>37</sup> on a seven-valence-electron pseudopotential with one d polarization function, denoted SECP, was used. All geometries were fully optimized and verified to be local minima on the potential energy surface by frequency calculations. Single-point energies were zero-point corrected.

## 3. Results and Discussion

**Density Functional Calculations.** To compare the data of the literature<sup>16</sup> with the results presented in this work and check the reliability of the chosen method and basis set, the anionic iodine–water cluster  $I^-(H_2O)$  was recalculated. A linear geometry for the hydrogen bond with  $C_s$  symmetry and an  $I \cdots H$  bond length of 2.68 Å was found to be the global minimum on the potential energy surface of  $I^-(H_2O)$ . With a scaling factor of 0.965, the calculated vibrational frequencies of 3408 and 3721  $cm^{-1}$  for the hydrogen-bonded OH stretch and the free OH stretch, respectively, are in excellent agreement with the experimental results of Johnson et al.<sup>16</sup> Their vibrational predissociation spectroscopy yielded 3415 and 3710  $cm^{-1}$ , respectively.

To further test the reliability of our computational approach, especially with regard to bond dissociation energies, we compared the two proton affinities of HOI at 0 K with the G2-(ECP) results by Glukhovtsev et al.<sup>24</sup> The values of 720 and 637 kJ/mol they report for protonation at the oxygen and iodine atoms, respectively, compare very favorably with our results of 717 and 629 kJ/mol. In both cases, the relative difference is of the order of 1%, and the absolute deviation lies within the “chemical error” of 8 kJ/mol. In our study, we optimize the geometry at the same level of theory at which the single-point energy calculations are done, while in G2 theory, geometries are optimized at a lower level of theory than that of the final energy calculations, which might cause these small deviations. However, considering how very different the G2 and DFT approaches are, the agreement is excellent.

Various optimized geometries of  $I(H_2O)_n^+$ ,  $n = 1–4$ , are displayed in Figure 1, together with key geometry parameters. All species are found to have singlet spin multiplicity. The ions exhibit structures consisting of a positively charged “central”  $H_2IO^+$  and  $H_4IO_2^+$  subunit, solvated by additional water ligands. This might be expected on the basis of the proton affinity of HOI, which is considerably higher than that of  $H_2O$ . Somewhat surprisingly, in the latter ion, not the small proton but the bulky iodine atom is found to be bridging the two water molecules.

The length of the I–O bond is found to depend sensitively on the local environment and on the state of solvation of the ion. In general, asymmetric solvation of the iodine tends to shorten the I–O bond length. Thus, while in the symmetric  $H_4IO_2^+$  cation **2** both bonds are 2.29 Å, in the  $H_2IO^+$

(24) Glukhovtsev, M. N.; Pross, A.; Radom, L. *J. Phys. Chem.* **1996**, *100*, 3498.

(25) Ghanty, T. K.; Ghosh, S. K. *J. Phys. Chem. A* **1997**, *101*, 5022.

(26) Hassanzadeh, P.; Irikura, K. K. *J. Phys. Chem. A* **1997**, *101*, 1580.

(27) Ma, N. L.; Cheung, Y. S.; Ng, C. Y.; Li, W. K. *Mol. Phys.* **1997**, *91*, 495.

(28) Thorn, R. P.; Stief, L. J.; Kuo, S. C.; Klemm, R. B. *J. Phys. Chem. A* **1999**, *103*, 812.

(29) Minaev, B. F. *J. Phys. Chem. A* **1999**, *103*, 7294.

(30) Berg, C.; Schindler, T.; Niedner-Schatteburg, G.; Bondybey, V. E. *J. Chem. Phys.* **1995**, *102*, 4870.

(31) Caravatti, P.; Allemann, M. *Org. Mass Spectrom.* **1991**, *26*, 514.

(32) Bondybey, V. E.; English, J. H. *J. Chem. Phys.* **1981**, *74*, 6978.

(33) Dietz, T. G.; Duncan, M. A.; Powers, D. E.; Smalley, R. E. *J. Chem. Phys.* **1981**, *74*, 6511.

(34) Becke, A. D. *Phys. Rev. A* **1988**, *38*, 3098.

(35) Becke, A. D. *J. Chem. Phys.* **1993**, *98*, 5648.

(36) Frisch, M. J.; Trucks, G. W.; Schlegel, H. B.; Gill, P. M. W.; Johnson, B. G.; Robb, M. A.; Cheeseman, J. R.; Keith, T.; Petersson, G. A.; Montgomery, J. A.; Raghavachari, K.; Al-Laham, M. A.; Zakrzewski, V. G.; Ortiz, J. V.; Foresman, J. B.; Cioslowski, J.; Stefanov, B. B.; Nanayakkara, A.; Challacombe, M.; Peng, C. Y.; Ayala, P. Y.; Chen, W.; Wong, M. W.; Andres, J. L.; Replogle, E. S.; Gomperts, R.; Martin, R. L.; Fox, D. J.; Binkley, J. S.; Defrees, D. J.; Baker, J.; Stewart, J. P.; Head-Gordon, M.; Gonzalez, C.; Pople, J. A. *Gaussian 94*, Revision D.4; Gaussian, Inc.: Pittsburgh, PA, 1995.

(37) Kaupp, M.; Schleyer, P.; Stoll, H.; Preuss, H. *J. Am. Chem. Soc.* **1991**, *113*, 6012. Dolg, M. *J. Chem. Phys.* **1989**, *91*, 1762.

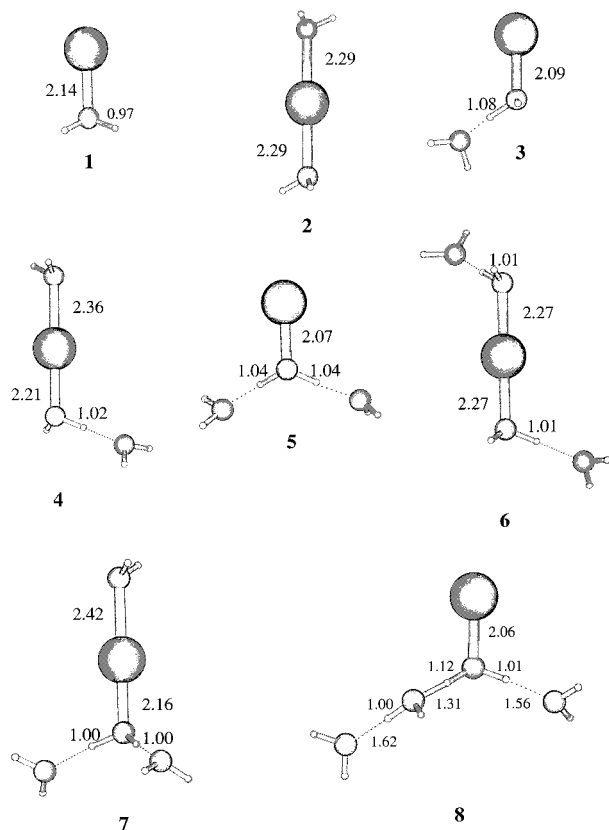


**Figure 1.** Fully optimized structures of  $I(H_2O)_n^+$ ,  $n = 1-4$ , at the B3LYP level of theory. Bond lengths are in angstroms. All O–H bonds, except where otherwise noted, are 0.97 Å.

monohydrate it is shortened to 2.14 Å. Additional asymmetric hydration shortens the I–O bond length further, from 2.09 Å in **3** over 2.07 Å in **5** to 2.06 Å in **8**. This shortening of I–O bond length is accompanied by a considerable elongation of the O–H bonds of the central ion. In structure **8**, one hydrogen bond even looks very much like a proton bond, with H–O bond lengths of 1.12 and 1.31 Å, instead of the more typical 1.00 and 1.56 Å on the less solvated side in the same cluster.

Similarly, additional asymmetric hydration of **2** by one or two water molecules shortens one I–O bond length to 2.21 Å in ion **4** and 2.16 Å in **7**, while at the same time the other one is lengthened to 2.36 and 2.42 Å, respectively. Apparently, the asymmetric solvation tends to localize the positive charge in the region of one of the I–O bonds, resulting in stronger binding and in bond shortening. A symmetrical substitution of **2** on both ends, on the other hand, has little effect on the I–O bonds, which are both only marginally shortened in **6** from 2.29 to 2.27 Å. The situation resembles very much the permanent transition from  $H_3O^+$  and  $H_5O_2^+$  in protonated water clusters, where, depending on the cluster size and state of solvation, one or the other structure is stabilized.<sup>38</sup> To make the situation even more complex, proton-bound structures emerge with more extreme asymmetric solvation, as can be seen in **8**. All these variations differ in energy by less than the contribution of a single hydrogen bond. The trends with increasing solvation are therefore impossible to predict.

The relative energies listed in Table 1 give some insight into the geometry trends. In general, the symmetrical species **2**, **4**, and **6** based on the  $H_4IO_2^+$  core are about 20 kJ/mol lower in energy than the asymmetric  $H_2IO^+$ -based isomers **3**, **5**, and **8**.

**Table 1.** Relative Energies Calculated at the B3LYP/6-311++G(3d,3pd)/SECP Level of Theory<sup>a</sup>

structure	relative energy, $\Delta E_0$ , kJ/mol
$H^+ + HOI + 3H_2O$	716.9
$I^+ + 4H_2O$	140.2
<b>1</b> + 3H <sub>2</sub> O	0
<b>2</b> + 2H <sub>2</sub> O	–137.7
<b>3</b> + 2H <sub>2</sub> O	–113.8
<b>4</b> + H <sub>2</sub> O	–213.0
<b>5</b> + H <sub>2</sub> O	–196.9
<b>6</b>	–276.7
<b>7</b>	–275.7
<b>8</b>	–255.2

<sup>a</sup> Structure numbering refers to Figure 1.  $H_2OI^+ + 3H_2O$  is defined as 0 kJ/mol.

**Table 2.** Natural Partial Charges on I and the Directly Coordinated O Atoms<sup>a</sup>

structure	I	O1	O2
HOI	0.379	–0.851	
<b>1</b>	0.664	–0.781	
<b>2</b>	0.550	–0.837	–0.837
<b>3</b>	0.592	–0.814	
<b>4</b>	0.524	–0.851	–0.855
<b>5</b>	0.549	–0.829	
<b>6</b>	0.504	–0.945	–0.945
<b>7</b>	0.504	–0.868	–0.871
<b>8</b>	0.520	–0.844	

<sup>a</sup> O1 is the oxygen with the shorter I–O bond length.

This difference is on the order of the energy of a single hydrogen bond and seems to decrease somewhat with the increasing number of ligands. It is possible that with the increasing cluster size, the formation of closed rings containing an  $H_2IO^+$  subunit may become more favorable. The natural partial charges<sup>39</sup> on I and neighboring O atoms, listed in Table 2, also illustrate the smooth transition and relative insensitivity of the iodine to its surroundings. Upon solvation, a partial charge of 0.50–0.55 e is stabilized on the iodine.

**Blackbody Radiation-Induced Fragmentation.** Fragmentation of the  $I(H_2O)_n^+$  clusters in the range up to  $n \approx 30$  was studied and found to consist of a simple, sequential loss of water ligands. In no case was a loss of iodine or HOI detected. By fitting the decay of the intensity of mass-selected iodine–water clusters as a function of time to first-order reaction kinetics, one obtains the fragmentation rate constants. The rates obtained in the present work in this way for the  $I(H_2O)_n^+$ ,  $n = 4-15$ , are shown as open circles in Figure 2 and compared in Table 3 with similar measurements for the anionic  $I^-(H_2O)_n$ ,  $n = 1-13$ .<sup>1</sup> The solid line in Figure 2 represents a linear regression of the data set. Both rate constants of iodine–water clusters follow roughly an overall linear increase with cluster size.

Each fit  $k = k_0(n - n_0)$  is characterized by a slope  $k_0$  and an abscissa intercept  $n_0$ . As discussed in detail previously,<sup>23</sup> the physical meaning of the slope  $k_0$  is the contribution of each solvent molecule to the infrared absorption from the blackbody background, and thus to the fragmentation rate. The intercept then reflects the fact that the strongly bound smallest clusters, even when they reach thermal equilibrium with the room-temperature walls, do not contain enough energy to fragment. The basis for the linearity of the plot is the assumption that, regardless of the size of the cluster, it takes about the same energy to evaporate one ligand. While this is apparently valid to a fair approximation for large clusters, those ligands that are

(38) Jiang, J. C.; Wang, Y. S.; Chang, H. C.; Lin, S. H.; Lee, Y. T.; Niedner-Schatteburg, G.; Chang, H. C. *J. Am. Chem. Soc.* **2000**, *122*, 1398.

(39) (a) Reed, A. E.; Curtiss, L. A.; Weinhold, F. *Chem. Rev.* **1988**, *88*, 899. (b) Lipkowitz, K. B.; Boyd, D. B. In *Reviews in Computational Chemistry*; VCH: New York, 1990; Vol. 5.



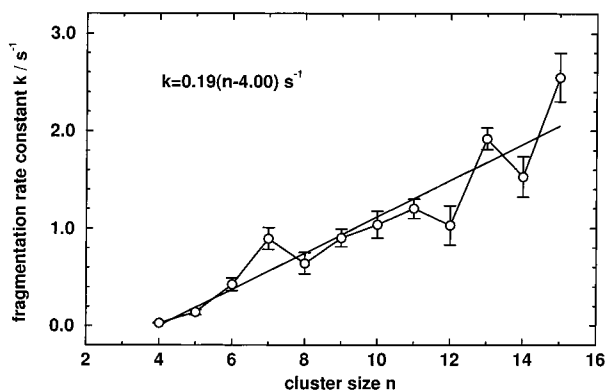


**Figure 2.** Unimolecular rate constants of the blackbody radiation-induced fragmentation process  $\text{I}(\text{H}_2\text{O})_n^+ \rightarrow \text{I}(\text{H}_2\text{O})_{n-1}^+ + \text{H}_2\text{O}$ .

**Table 3.** Unimolecular Rate Constants  $k$  of Blackbody Radiation-Induced Fragmentation of  $\text{I}(\text{H}_2\text{O})_n^\pm$  Clusters<sup>a</sup>

$n$	$k [\text{I}^-(\text{H}_2\text{O})_n], \text{s}^{-1}$	$k [\text{I}(\text{H}_2\text{O})_n^+], \text{s}^{-1}$
1	$0.03 \pm 0.003$	
2	$0.07 \pm 0.003$	
3	$0.17 \pm 0.03$	
4	$0.40 \pm 0.05$	$0.03 \pm 0.004$
5	$0.53 \pm 0.06$	$0.14 \pm 0.03$
6	$0.62 \pm 0.04$	$0.43 \pm 0.07$
7	$0.87 \pm 0.10$	$0.90 \pm 0.11$
8	$1.37 \pm 0.13$	$0.64 \pm 0.11$
9	$1.23 \pm 0.15$	$0.90 \pm 0.09$
10	$1.20 \pm 0.15$	$1.04 \pm 0.14$
11	$1.90 \pm 0.3$	$1.20 \pm 0.10$
12	$1.60 \pm 0.3$	$1.15 \pm 0.10$
13		$1.92 \pm 0.11$
14		$1.53 \pm 0.21$
15		$2.55 \pm 0.25$

<sup>a</sup> Rate constants for  $\text{I}^-(\text{H}_2\text{O})_n$  are taken from ref 1.

**Table 4.** Slope and Abscissa Intercept of the Linear Regression  $k = k_0(n - n_0)$  Evaluated for Different Core Ions and the Terminal Product of Each Fragmentation Process

$\text{X}(\text{H}_2\text{O})_n^\pm$	slope $k_0$	intercept $n_0$	terminal product
$\text{H}^+, n = 5-65$	$0.20 \pm 0.01$	1.39	$\text{H}(\text{H}_2\text{O})_4^+$
$\text{Al}^+, n = 4-11, 25-45$	$0.16 \pm 0.01$	1.63	$\text{Al}(\text{OH})_2(\text{H}_2\text{O})_3^+$
$\text{Ag}^+, n = 4-45$	$0.18 \pm 0.01$	5.31	$\text{Ag}(\text{H}_2\text{O})_3^+$
$\text{Mg}^+, n = 2-41$	$0.17 \pm 0.01$	2.35	$\text{MgOH}(\text{H}_2\text{O})_4^+$
$\text{I}^+, n = 1-15$	$0.19 \pm 0.02$	4.00	$\text{I}(\text{H}_2\text{O})_3^+$
$\text{I}^-, n = 1-12$	$0.17 \pm 0.01$	1.53	$\text{I}^-$

in direct contact with the ionic central ion are much more strongly bound, and this is obviously reflected in strong deviation from linearity, and eventually in the intercept  $n_0$  when one attempts a linear fit of the experimental data. Both the slope and intercept, of course, depend on the range of sizes included in the fit. They should naturally also exhibit some dependence on the central ion, and we compare in Table 4 the fit parameters obtained in the present work for the iodine cation and anion clusters with those obtained for a number of other hydrated cations.<sup>1,21,23,40,41</sup> The comparison shows that the slopes are, for all the systems studied, remarkably similar, about  $0.17 \pm 0.01 \text{ s}^{-1}$ . This simply reflects the facts that (a) beyond the first or perhaps second solvation shell, the binding energies of the water molecules are basically similar and independent of the central ion, and (b) the contribution of a water ligand to the rate of absorption and to the total energy of the cluster is not strongly dependent on the central ion.

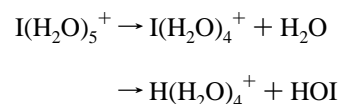
(40) Berg, C.; Beyer, M.; Achatz, U.; Joos, S.; Niedner-Schatteburg, G.; Bondybey, V. E. *Chem. Phys.* **1998**, 239, 379.

(41) Beyer, M.; Achatz, U.; Berg, C.; Joos, S.; Niedner-Schatteburg, G.; Bondybey, V. E. *J. Phys. Chem. A* **1999**, 103, 671.

When one compares the hydrated iodine anions and cations, there is a considerable difference in the final stages of the fragmentation and in the observed final products. While in the anionic case the clusters fragment down to the naked  $\text{I}^-$  ion, for the cationic clusters three water molecules remain on the iodine on the time scale of the ICR experiment. This difference is already evidenced by the fit parameter  $n_0$  in Table 4, which has a value of 4.00 for the cation but only 1.53 for the anions.

The different terminal ions,  $\text{I}^-$  and  $\text{I}(\text{H}_2\text{O})_3^+$ , reflect the fact that the binding energy of a water molecule to the iodide ion is smaller than the ligand binding energies in the cationic species. In anions, the charge is, in general, much more diffuse than in cations. Furthermore, in the anionic clusters, the dipole of the water molecules is not collinear with the bond, thus reducing the charge-dipole interaction. The calculations show that, in the  $\text{H}_4\text{IO}_2^+$  ion, the two water molecules are bridged by the iodine atom, forming a symmetric molecular ion comparable to  $\text{H}_5\text{O}_2^+$ , with strong covalent bonds. As was outlined previously,<sup>22,23</sup> the fragmentation will come to an end when the internal energy of the cluster at room temperature is no longer sufficient to break the weakest bond, with the binding energy of the ligands being the key parameter. Our calculations indicate that, while only 38.6 kJ/mol is required to dissociate  $\text{I}^-(\text{H}_2\text{O})$ , 75.4 kJ/mol is needed to remove a water ligand from  $\text{I}(\text{H}_2\text{O})_3^+$ , clearly explaining the difference in behavior.

At first, the experimental observation that no loss of HOI is detected might seem to contradict the notion that the cluster might be viewed as a protonated water cluster with an HOI "impurity" ligand. However, a different picture emerges if one considers the proton affinity of the HOI molecule. The energy of protonation on the oxygen atom of HOI has been calculated previously<sup>24,25</sup> and lies at 724.7 kJ/mol, well above the experimentally known proton affinity of water, 691.0 kJ/mol.<sup>42</sup> The proton would therefore undoubtedly remain on the HOI during the fragmentation process. This was further confirmed by comparison of the relative stabilities of  $\text{I}(\text{H}_2\text{O})_4^+$ , structure **6**, and  $\text{H}(\text{H}_2\text{O})_4^+$ . The fragmentation of  $\text{I}(\text{H}_2\text{O})_5^+$  can, in principle, proceed in two different ways, by evaporation of a water molecule or by loss of HOI:



We have calculated the  $\text{H}(\text{H}_2\text{O})_4^+$  on the same level of theory as the  $\text{I}(\text{H}_2\text{O})_n^+$  clusters and found by comparison of the total energies of the right-hand sides that evaporation of  $\text{H}_2\text{O}$  is thermochemically favored by 12.0 kJ/mol. This illustrates that, in the present case, solvation reduces the difference in proton affinity, but nevertheless, a strong thermochemical preference for evaporation of  $\text{H}_2\text{O}$  against HOI prevails.

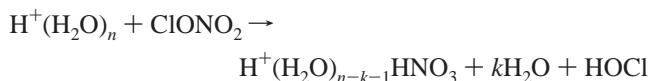
On the other hand, the calculated proton affinities for the other hypohalous acids HOF, HOCl, and HOBr all lie below the proton affinity of water,<sup>24</sup> and it is therefore of interest to consider if protonated water clusters with, e.g., HOBr or HOCl impurity can be produced at all, and whether the lighter hypohalite molecules would evaporate at a certain critical size.

Some time ago, we examined the hydrolysis of chlorine nitrate catalyzed by ionic water clusters,<sup>43</sup> a reaction which is of considerable importance in stratospheric chemistry and ozone destruction. The reaction proceeds with fairly high efficiency,

(42) Lias, S. G.; Bartmess, J. E.; Liebman, J. F.; Holmes, J. L.; Levin, R. D.; Mallard, W. G. *J. Phys. Chem. Ref. Data* **1988**, 17, Suppl. 1.

(43) Schindler, T.; Berg, C.; Niedner-Schatteburg, G.; Bondybey, V. E. *J. Chem. Phys.* **1996**, 104, 3998.

yielding hypochlorous acid and nitric acid:



While the nitric acid in most cases remains “dissolved” in the aqueous clusters, the HOCl is usually evaporated into the gas phase, as suggested by the above discussion and its lower proton affinity. Only with a very low efficiency do products containing chlorine form, and even in these cases the hypochlorous acid is lost at a later stage of the fragmentation.

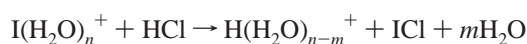
**Reactions with HCl.** As in our previous study of hydrated  $\text{I}^-$  anions, we have also investigated the reaction of the hydrated cations with hydrochloric acid. In these experiments, HCl at a pressure of  $1.0 \times 10^{-8}$  mbar was admitted into the cell region, and the products were examined after varying reaction delays. In our previous study of anions,<sup>1</sup> only ligand exchange and gradual fragmentation were observed, with ultimately all of the water ligands being lost. After longer delays, only iodide anions solvated by several HCl molecules were found, which gradually fragmented by loss of HCl molecules.

As one might expect from the discussion of the significantly different structures, the reactions of the  $\text{I}(\text{H}_2\text{O})_n^+$  cation clusters in the present study are found to be considerably different. Figure 3 follows the reaction of the  $\text{I}(\text{H}_2\text{O})_n^+$  cations in the size range  $n = 9-25$  with HCl. The interpretation is somewhat complicated by the fact that the initial distribution at the nominal  $t = 0$  time contains not only the  $\text{I}(\text{H}_2\text{O})_n^+$  species, but a variety of other clusters. Thus, for instance, in the experiment shown in Figure 3, besides  $\text{I}(\text{H}_2\text{O})_n^+$ ,  $n \approx 9-25$ , also  $\text{H}(\text{H}_2\text{O})_n^+$ ,  $n \approx 7-31$ , species are present, as well as minor impurity clusters containing  $\text{Na}^+$ . Also, due to the relatively long,  $\sim 2$  s accumulation time, HCl-containing products, e.g., of the type  $\text{H}(\text{H}_2\text{O})_{n-2m}(\text{HCl})_m^+$ , have already been formed. Even though clusters  $\text{H}(\text{H}_2\text{O})_n^+$ ,  $\text{I}(\text{H}_2\text{O})_{n-7}^+$ , and  $\text{H}(\text{H}_2\text{O})_{n-2m}(\text{H}^{35}\text{Cl})_m^+$  accidentally all have same nominal masses, this turns out not to be a problem, as the resolution of the instrument is adequate to clearly distinguish between them on the basis of the mass defect over the entire mass range studied. Furthermore, the isotopic pattern provides a clear “fingerprint”, revealing how many chlorine atoms a given cluster contains.

Comparison of the “time 0” distribution in Figure 3a with the “final” one in panel d reveals that, while initially the iodine-containing ions represented some 50% of the total, after 15 s less than 15% iodine-containing clusters remain, with more than 85% of the final distribution being hydrated protons. Figure 4 displays the relative intensities of the two cluster series as a function of time. Clearly, with increasing reaction delay, the intensity of protonated water clusters increases at the expense of iodine-containing species. Interestingly, no clusters containing both iodine and chlorine are detected. The observed stoichiometry would permit a ligand exchange reaction of the type



In view of the much higher proton affinity of HOI as compared to that of  $\text{H}_2\text{O}$ , however, as discussed above, this appears unlikely. More reasonable is the following primary reaction step:



Indeed, the reverse of this reaction is well known from bulk

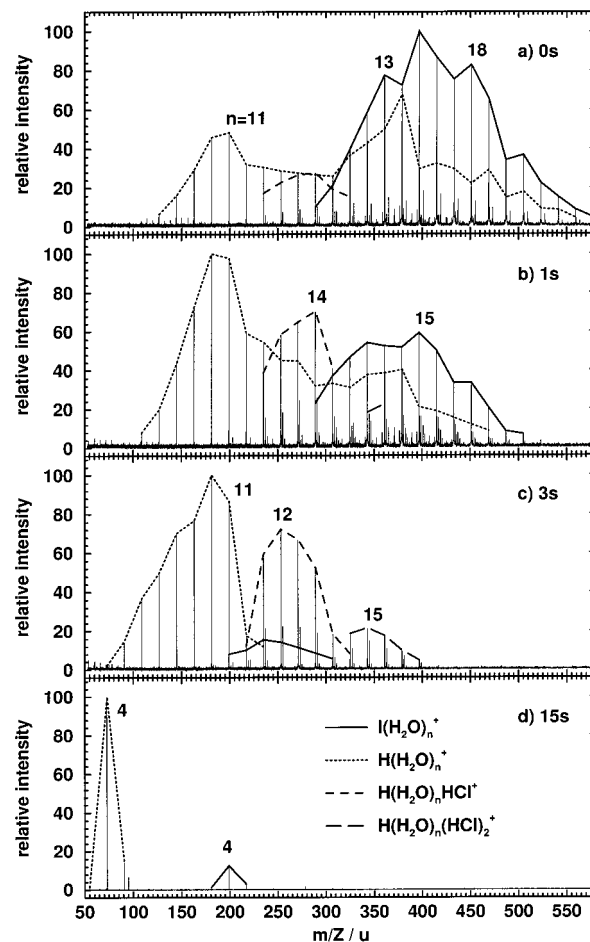
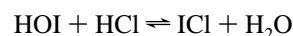


**Figure 3.** Mass spectra of the reaction of iodine–water clusters  $\text{I}(\text{H}_2\text{O})_n^+$ ,  $n = 9-25$ , and  $\text{H}^+(\text{H}_2\text{O})_m$ ,  $m = 7-31$ , with HCl at a pressure of about  $10^{-8}$  mbar in the cell region after variable reaction delays.  $\text{I}(\text{H}_2\text{O})_n^+$ ,  $n \leq 10$ , only show blackbody radiation- and collision-induced fragmentation reactions, while larger clusters with  $n \geq 11$  efficiently react, producing  $\text{H}^+(\text{H}_2\text{O})_{n-x}$  and releasing the intra-halide ICl into gas phase. Subsequent reactions of  $\text{H}^+(\text{H}_2\text{O})_n$  with HCl result in  $\text{H}^+(\text{H}_2\text{O})_m(\text{HCl})_k$ ,  $k = 1, 2$ , which again lose HCl at the critical size,  $m = 11$ .

solutions<sup>44</sup> as hydrolysis of interhalogen compounds:



Given the strong acidity of the cluster, one proton per 55 water molecules amounts to  $\text{pH} = 0$ , the equilibrium in the cluster must lie far on the ICl side.

From previous studies of protonated water clusters with HCl by our group,<sup>5</sup> it was established that HCl leaves a protonated water cluster in the fragmentation process at  $n = 11$ , and conversely, at least 11 water molecules are needed to dissolve one HCl in a protonated water cluster  $\text{H}(\text{H}_2\text{O})_n^+$ . The data in Figure 4 suggest that a similar boundary exists for ionic dissolution of HCl in  $\text{I}(\text{H}_2\text{O})_n^+$ . Comparing the total intensities of  $\text{I}(\text{H}_2\text{O})_n^+$  and products in Figure 3a with the intensities of the final products in Figure 3d, one can estimate that  $n \geq 11$  water molecules are again needed to dissolve HCl. Since furthermore one or two water ligands will be lost upon the intake of HCl, only  $\text{I}(\text{H}_2\text{O})_n^+$  with  $n \geq 13$  may react efficiently with HCl. The presence of protonated water clusters  $\text{H}(\text{H}_2\text{O})_n^+$  starting with  $n = 8$  in Figure 3a may be interpreted by the

(44) Hollemann, A. F.; Wiberg, E. *Lehrbuch der Anorganischen Chemie*, 101 Auflage; Walter de Gruyter: Berlin, 1995.

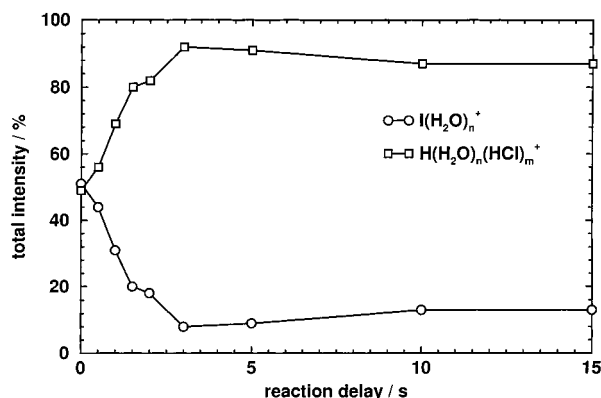
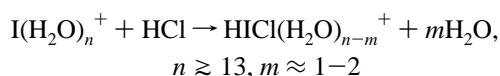


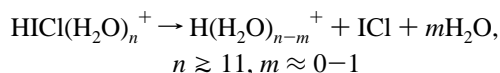
**Figure 4.** Relative ion intensity versus reaction delay of  $I(H_2O)_n^+$  and  $H(H_2O)_n(HCl)_m^+$ ,  $m = 0-2$ . The reaction to form  $H(H_2O)_n^+$  is complete after 3 s reaction delay. Afterward, only subsequent blackbody radiation and collision-induced fragmentation takes place. Errors are estimated to lie within 10%.

following reaction sequence:

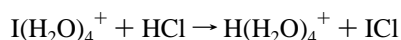
Intake of HCl:



Formation of ICl:



Apparently, the elimination of ICl must occur fast compared with the millisecond time scale of the FT-ICR experiment, so that no intermediates containing both chlorine and iodine are observed. In the gas phase, the reaction  $HOI + HCl \rightarrow ICl + H_2O$  is calculated to be exothermic by  $-60.3$  kJ/mol. With the largest clusters calculated in this work, the effect of solvation can be estimated by evaluating the thermochemistry of the cluster reaction:



This reaction is still exothermic by  $-48.3$  kJ/mol, which is sufficient to break two or three hydrogen bonds or to evaporate about two water molecules from the cluster.

In subsequent reactions, the  $H(H_2O)_n^+$ ,  $n \gtrsim 11$ , as previously observed,<sup>5</sup> ionically dissolve HCl and form the  $H(H_2O)_n(HCl)_m^+$  products, which in turn lose HCl at defined cluster sized during the fragmentation.

#### 4. Conclusion

Unimolecular fragmentation rates of  $I(H_2O)_n^+$ ,  $n = 1-15$ , by ambient temperature blackbody radiation under collision-free conditions, exhibit a roughly linear dependence on cluster size  $n$ , similar to what was observed for other hydrated clusters. Unlike the hydrated anions, which yield bare  $I^-$ , fragmentation of cations results in  $I(H_2O)_3^+$  as the final product. The differences are explained with the help of accompanying ab initio calculations, in terms of a pronounced difference in the stepwise solvation energies. The cation clusters are found to consist of a  $H_2IO^+$  and  $H_4IO_2^+$  ionic core solvated by additional water ligands. Similar to the case for  $H_3O^+$  and  $H_5O_2^+$  in protonated water clusters, the relative stability of the core ions depends on the cluster size and solvation. The positive charge is localized in the vicinity of the iodine, reflecting the high proton affinity of HOI. The  $H_4IO_2^+$  is bridged by the iodine, and proton-bound structures may develop with increasing asymmetric solvation.

Chemical reactions with hydrochloric acid were investigated. While smaller cationic iodine-water clusters  $I(H_2O)_n^+$ ,  $n \leq 10$  only fragment and lose the water ligands, the larger species with  $n \gtrsim 11$  react chemically, releasing the ICl interhalogen, and resulting in hydrated proton clusters. Unlike HOI, the proton affinities of HOBr and HOCl are lower than that of water, which is consistent with our earlier observation that HOCl evaporates readily and preferentially from water clusters. Further study of the production and chemistry of hydrated  $Br(H_2O)_n^+$  or  $Cl(H_2O)_n^+$  and the question of HOBr or HOCl elimination would seem to be an interesting topic for further experimental and theoretical studies.

**Acknowledgment.** Financial support by the Deutsche Forschungsgemeinschaft and the Fonds der Chemischen Industrie is gratefully acknowledged.

**Supporting Information Available:** Optimized geometries in Cartesian coordinates, calculated harmonic frequencies with infrared intensities, and thermochemical values of all calculated species (PDF). This material is available free of charge via the Internet at <http://pubs.acs.org>.

JA010381W